**Original Article**
J Vet Sci 2016, 17(2), 235-242 · http://dx.doi.org/10.4142/jvs.2016.17.2.235

# Hematoporphyrin monomethyl ether combined with He–Ne laser irradiation-induced apoptosis in canine breast cancer cells through the mitochondrial pathway

Huatao Li[1,2], Jinjin Tong[1], Jun Bao[3,4], Damu Tang[5], Wenru Tian[2], Yun Liu[1,*]

[1]*Department of Clinic Veterinary Medicine, College of Veterinary Medicine,* [3]*College of Animal Science and Technology, and* [4]*Synergetic Innovation Center of Food Safety and Nutrition, Northeast Agricultural University, Harbin 150030, China*
[2]*Department of Veterinary Medicine, College of Animal Science and Veterinary Medicine, Qingdao Agricultural University, Qingdao 266109, China*
[5]*Department of Medicine, McMaster University, Hamilton, L8S 4L8, Canada*

Hematoporphyrin monomethyl ether (HMME) combined with He-Ne laser irradiation is a novel and promising photodynamic therapy (PDT)-induced apoptosis that can be applied *in vitro* on canine breast cancer cells. However, the exact pathway responsible for HMME-PDT in canine breast cancer cells remains unknown. CHMm cells morphology and apoptosis were analyzed using optical microscope, terminal deoxynucleotidyl transferase dUTP nick end labeling fluorescein staining and DNA ladder assays. Apoptotic pathway was further confirmed by Real-time-polymerase chain reaction and Western blotting assays. Our results showed that HMME-PDT induced significant changes in cell morphology, such as formation of cytoplasmic vacuoles and the gradual rounding of cells coupled with decreased size and detachment. DNA fragmentation and cell death was shown to occur in a time-dependent manner. Furthermore, HMME-PDT increased the activities of caspase-9 and caspase-3, and released cytochrome c from mitochondria into the cytoplasm. HMME-PDT also significantly increased both mRNA and protein levels of Bax and decreased P53 gene expression in a time-dependent manner, while the mRNA and protein expression of Bcl-2 were repressed. These alterations suggest that HMME-PDT induced CHMm cell apoptosis via the mitochondrial apoptosis pathway and had anti-canine breast cancer effects *in vitro*.

**Keywords:** CHMm cells, apoptosis, hematoporphyrin monomethyl ether, mitochondrial pathway, promising photodynamic therapy

## Introduction

Photodynamic therapy is an effective method to treat malignant tumors [4] that can deactivate malignant cells via reactive oxygen species (ROS) produced by light-activated photosensitizers. During promising photodynamic therapy (PDT), tumor cells absorb and accumulate a large number of photosensitizers, resulting in PDT-induced lesions in malignant tumor tissues [33]. Preclinical and clinical trials have shown that PDT results in formation of malignancies at multiple sites with minimal normal tissue toxicity [29]. Photodynamic therapy is a minimally invasive treatment that can be used repeatedly at the same site. Moreover, PDT can be utilized in combination with chemotherapy, ionizing radiation, or surgery, making it a promising treatment option for adjuvant tumor therapy.

Selection of appropriate animal models for human breast tumors remains a major challenge in advancing breast cancer research. Canine and human mammary glands share similar molecular mechanisms [14]. For example, spontaneous tumors in dogs possess many similar features as those found in humans, including relevant biological behavior, histological appearance, molecular targets, genetics and response to conventional treatments [15]. Moreover, molecular cytogenetic analyses have shown that canine and human tumor cells derived from hematological malignancies preserve the ancestral chromosomal aberrations [2,34]. The expression of *ERBB2* and *TP53* genes demonstrated similar alterations in mammary carcinomas in dogs and human, indicating they have similar roles in carcinogenesis and potential prognostic index [10,31]. Moreover, dogs have a relatively large body size when compared with other laboratory animals, in addition to

Received 21 Jan. 2015, Revised 26 Aug. 2015, Accepted 7 Oct. 2015
*Corresponding author: Tel: +86-451-55190150; Fax: +86-451-55190150; E-mail: abliuyun@yeah.net
pISSN 1229-845X
eISSN 1976-555X

providing genetic diversity similar to humans. Therefore, dogs are an attractive potential model for human cancer research [28,35].

Hematoporphyrin monomethyl ether (HMME) is a promising photosensitizer that has been of great interest to researchers because of its advantageous physicochemical properties [5,33]. HMME combined with a He-Ne laser as a novel treatment demonstrated a great advantage in the potential treatment of canine breast cancer [18,19]. Previous studies have shown that HMME-PDT could induce the death of canine breast cancer cells through apoptosis *in vitro* [19] via damage to the mitochondrial structure and dysfunction [18]; however, the detailed mechanism underlying HMME-PDT induced apoptosis through the mitochondrial pathway remains unclear. Therefore, this study was conducted to investigate the relationship of HMME-PDT induced apoptosis, cell morphology and gene expression with mitochondrial pathways of apoptosis.

## Materials and Methods

### Reagents and HMME-PDT

HMME was purchased from Red Green Photosensitizer (China). The He–Ne laser, CHMm cell line and cell culture conditions were described in a previous study [18,19,24]. Experimental cells were randomly divided into mock treatments (without HMME or irradiation), HMME (16 mM), irradiated ($2.8 \times 10^4$ J/m$^2$), or HMME (16 mM) plus laser irradiation ($2.8 \times 10^4$ J/m$^2$). Cells were cultured for 24 h, then pretreated with or without HMME with serum free medium for 2 h and irradiated with He-Ne laser according to the experimental plan. Subsequent analyses were carried out at 3 h, 6 h, 12 h, 24 h and 48 h post-irradiation.

### Terminal deoxynucleotidyl transferase dUTP nick end labeling (TUNEL) assay

Cells were plated at densities of $1.0 \times 10^5$ cells/cm$^2$ in 35-mm culture dishes with coverslips. Cells were washed three times with cold phosphate-buffered saline (PBS) after the selected treatment periods, then fixed for 10 min at −20°C in acetone/methanol (1 : 1, v/v). Apoptotic cell death was subsequently detected by the TUNEL method using commercial kits (KeyGen TUNEL Detection Kit; KeyGen, China) according to the manufacturer's protocols. Finally, cells were washed three times with cold PBS, then mounted on glass slides and dipped into emulsion and glycerol/PBS (1 : 3, v/v) to measure their fluorescence. The cells were visualized and analyzed using a Ti-s fluorescence microscope (Leica, Germany). Cells with apoptosis in the group panel were quantified by randomly counting 200 positively stained cells.

### DNA fragmentation

Samples ($3 \times 10^6$ cells) were collected from each group to measure DNA fragmentation. Fragmented DNA was isolated following the protocol described by Moore and Matlashewski [23]. Briefly, DNA pellets were washed once with 80% ethanol, spun down and air-dried, then dissolved in Tris-EDTA buffer at pH 7.6. Electrophoresis was performed on a 1.5% agarose gel for 1 h at 85 V. The results were analyzed and recorded with an Ultra Violet Products Gel Documentation System (ZF-208; Shanghai Jia Peng Technology, China).

### Measurement of cytochrome c release

Cells were harvested and washed twice with PBS for the cytochrome c release assay [17]. The cells were then incubated with extraction buffer (10 mM Hepes, 1.5 mM $MgCl_2$, 10 mM KCl, 250 mM sucrose, 1 mM EGTA, 1 mM EDTA, 0.05% digitonin, and 1 mM phenylmethylsulfonylfluoride) at 4°C for 10 min, then centrifuged at 100,000 × g for 10 min at 4°C. The supernatant represented the cytosolic extract. The pellet was subsequently disrupted in lysis buffer (1 mM EGTA, 1% Triton X-100, 10 mM Tris–HCl, pH 7.4, 1 mM EDTA, and protease inhibitors) to obtain a mitochondrial fraction. Finally, cytosolic or mitochondrial fractions were detected by Western blot and analyzed for cytochrome c.

### Western blot analysis

Cells were harvested and disrupted in 1 mL of cell lysis buffer (1% Triton X-100, 0.015 M NaCl, 10 mM Tris–HCl, 1 mM EDTA, 1 mM PMSF, 10 g/mL of each leupeptin and pepstain A) and incubated for 20 min on ice. Lysates were then centrifuged at 10,000 × g and 4°C for 20 min, after which the supernatants were mixed with one-quarter volume of 4× sodium dodecyl sulfate (SDS) sample buffer, boiled for 5 min and separated through a 12% SDS-polyacrylamide gel electrophoresis gel. After electrophoresis, proteins were blotted onto nylon membranes following the manufacturer's instructions (Bio-Rad Laboratories, USA). Next, membranes were blocked in 5% dry skim milk (1 h), rinsed and incubated with primary and secondary antibodies for 1 h at room temperature. Finally, Western Blots were quantified using an enhanced chemiluminescence system (GE Healthcare, USA). Densitometry of the Western blots was analyzed using the QuantiScan software (Biosoft, UK).

### Caspase-3 and caspase-9 activity assay

Enzymatic activity of caspase-3 and caspase-9 were detected using caspase-3 and caspase-9 activity assay kits (KeyGen) according to the manufacturer's protocols. Briefly, samples were collected and washed twice with ice-cold PBS, then re-suspended in 50 μL of chilled cell lysis buffer and incubated on ice for 30 min. Next, samples were centrifuged at 100,000 × g and 4°C for 10 min. The cytosolic extracts were then

transferred and kept on ice until the protein concentration was determined by BCA assay [36]. Briefly, protein samples (100 μg) were diluted with appropriate volumes of cell lysis buffer and 50 μL of 2× reaction buffer (containing 10 mM dithiothreitol) to a final volume of 100 μL. Caspase-3 or caspase-9 substrate (5 μL) was then added, after which samples were incubated at 37°C for 4 h. Finally, the caspase-3 or caspase-9 activity was assessed based on the absorbance at 405 nm using a microplate reader (Bio-Rad Laboratories).

### Real-time polymerase chain reaction (PCR) assay

Total RNA was isolated using TRIZOL reagent (Invitrogen, USA), after which template cDNA for real-time PCR was synthesized using the PrimeScript real time-PCR Kit (Takara Bio, Japan) according to the manufacturer's instructions. Quantitative real-time PCR was conducted using a LightCycler (Roche, Germany) with the SYBR Premix Ex Taq real time-PCR Kit (Takara Bio), LightCycler Fast Start DNA Master SYBR Green I (Takara Bio) and the following primers: β-actin (GenBank accession No. Z70044; forward: GCTGTCCTGTCCCTGTATTCC; reverse: AGCCAAGTCCA GACGACGCAAG), Bax (GenBank accession No. NM_001003011.1; forward: TTGCTTCAGGGTTTCTTCCA; reverse: CGACATTCGCTCCGCTTCTTG), Bcl-2 (GenBank accession No. NM_001002949; forward: CTTCGCCGTGATG TCCAG; reverse: CAGATGCGGGTTCAGATAC) and P53 (GenBank accession No. NM_001003210; forward: AAGA CCTACCCTGGCACCT; reverse: ACCTCGCTCACGAACT CC) according to the manufacturer's protocols. Gene expression was analyzed using the LightCycler software package. Relative gene expression was normalized to that of the housekeeping gene, β-actin, using the protocol described by MW Pfaffl [27].

### Statistical analysis

Data are expressed as the means ± SD. Differences between groups were evaluated by one-way ANOVA followed by a Student's *t* test using SPSS software (ver. 13.0; SPSS, USA). A difference at $p < 0.05$ was considered statistically significant.

## Results

### HMME-PDT induces apoptosis in canine breast cancer cells

The toxicity of HMME-PDT toward CHMm cells was observed by microscopy. The results revealed that HMME-

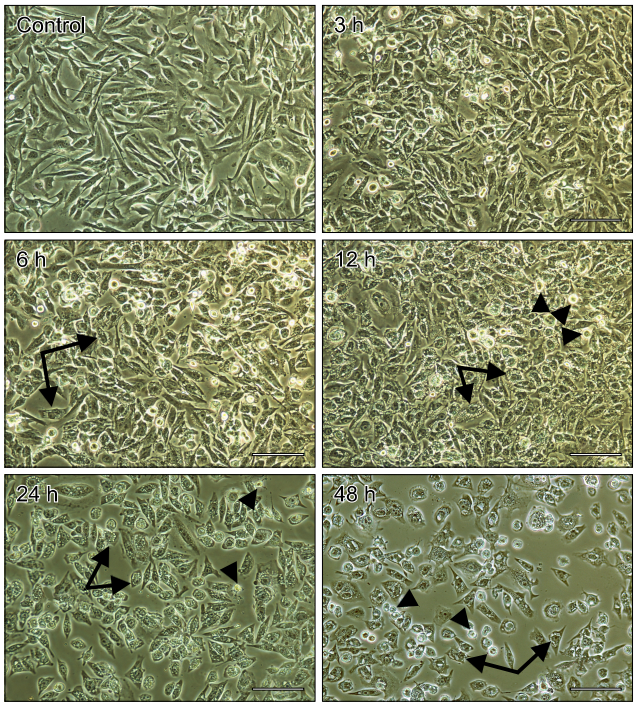


**Fig. 1.** Changes in cell morphology determined following hematoporphyrin monomethyl ether (HMME)-promising photodynamic therapy (PDT) treatment. CHMm cells were treated as indicated, after which images were acquired using a light microscope. Arrows indicate cells contained cytoplasmic vacuoles. Arrowheads show cells became round and smaller and detached. Scale bars = 100 μm.

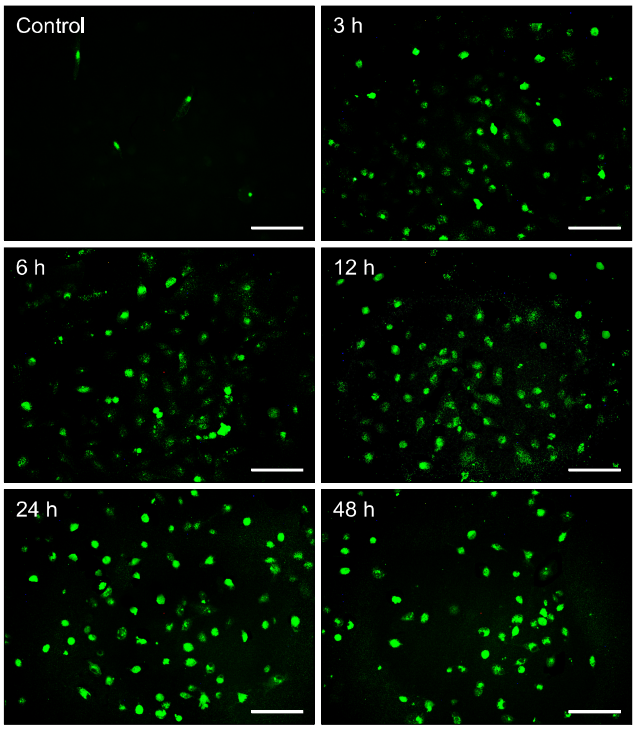


**Fig. 2.** TUNEL fluorescein staining to detect DNA fragmentation in CHMm cells following PDT–HMME treatment. Green fluorescence indicates DNA fragmentation. HMME-PDT treatments resulted in increased numbers of TUNEL-positive cells at all tested time points (6, 12, 24 and 48 h). Scale bars = 100 μm.

PDT caused morphological changes in cells at different time points after individual treatments (Fig. 1). When compared with mock treated cells, the growth of cells treated with HMME-PDT was significantly inhibited. Consistent with this observation, HMME-PDT treated cells demonstrated significantly more morphological changes than mock treated cells. A large number of HMME-PDT treated cells contained cytoplasm vacuoles (arrows in Fig. 1), and cells gradually became round, smaller and detached (arrowheads in Fig. 1). Cell death occurred in a time-dependent manner, showing sharply increased cell death and reduced density after 12 h of HMME and irradiation treatment relative to mock treated cells (Fig. 1).

TUNEL staining was used to detect apoptosis induced by HMME-PDT in canine breast cancer cells. The nuclei of apoptosis cells (TUNEL-positive cells) were labeled with fluorescein isothiocyanate, and their morphologic alterations associated with apoptosis were verified by fluorescence microscopy (Fig. 2). Apoptosis cells appearances at all tested time points (3, 6, 12, 24 and 48 h) post-exposure, and increased the rate induced by HMME-PDT. The apoptotic percentages of canine breast cancer cells after HMME-PDT treatment increased substantially (Table 1).

Apoptosis was also examined by DNA ladder analysis. A typical DNA ladder first responded to HMME-PDT at 3 h post-exposure, then became more prominent with time after exposure (Fig. 3).

Mitochondria Cyto C release was detected in cytosol using Western Blotting with a specific antibody. Western blot analysis showed that mitochondria Cyto C was released and induced by HMME-PDT at 6, 12, 24, and 48 h after irradiation (panel A in Fig. 4). Cyto C accumulated in a time-dependent manner in the cytosol (panel A in Fig. 4).

Since the release of Cyto C is linked with the activity of caspase-9 and caspase-3 in the mitochondrial apoptosis pathway, the enzymatic activity of caspase-9 and caspase-3 after HMME-PDT treatment was measured to understand the mechanism of cellular death. The activities of caspase-9 and caspase-3 were stimulated remarkably from 6 h and 12 h, respectively, relative to mock treated cells (panels B and C in Fig. 4).

**Relative gene and protein expression in the mitochondrial apoptotic pathway**

To investigate this, we monitored the expression of three important apoptosis-related genes (P53, Bax and Bcl-2) in CHMm cells challenged by HMME-PDT (Fig. 5). The P53 mRNA expression of HMME-PDT treated cells was significantly higher than that in the control treatment. Moreover, treatment with HMME-PDT up-regulated the mRNA and protein expression of Bax and down-regulated those of Bcl-2, resulting in a decreased Bcl-2 to Bax ratio (panel A in Fig. 5 and panel B in Fig. 5). The Bcl-2/Bax ratio of mRNA expression ranged from 0.8 to 0.09 and the protein expression ratio ranged from 1.2 to 0.14, indicating increased levels of apoptotic molecules in response to HMME-PDT (panel C in Fig. 5).

## Discussion

HMME-PDT induces canine breast cancer cell death via oxidative imbalance [20]. In the presence of oxygen, visible

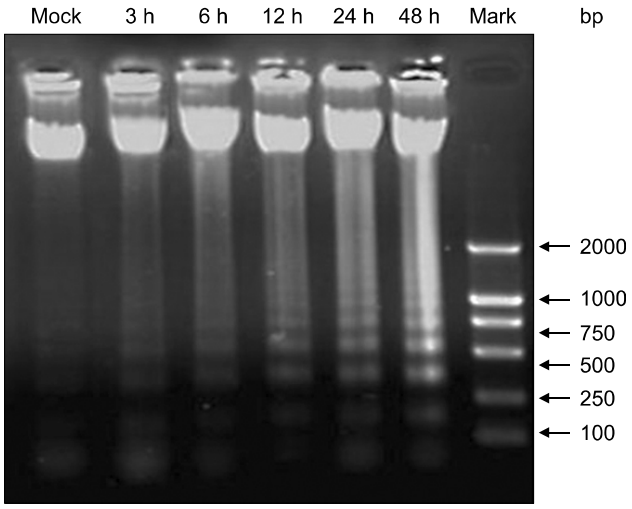


**Fig. 3.** DNA ladder assays detected DNA fragmentation in CHMm cells following PDT-HMME treatment. The ladder indicates DNA fragmentation. The ladder appeared first at 3 h after exposure, then became increasingly prominent with lengthening of exposure time.

**Table 1.** Apoptosis ratio of CHMm cells treated with HMME-PDT

| Group | Apoptosis ratio (mean ± SD, %) | | | | |
|---|---|---|---|---|---|
| | 3 h | 6 h | 12 h | 24 h | 48 h |
| Mock | 5.4 ± 0.53 | 5.7 ± 1.23 | 6.18 ± 2.42 | 5.9 ± 1.97 | 7.7 ± 3.48 |
| HMME-PDT | 11.1 ± 1.56* | 35.7 ± 1.43** | 68.8 ± 3.52** | 85.4 ± 2.07** | 87.7 ± 2.27** |

Asterisks statistically significant (*$p < 0.05$ and **$p < 0.01$, respectively) when compared to mock-treated cells.

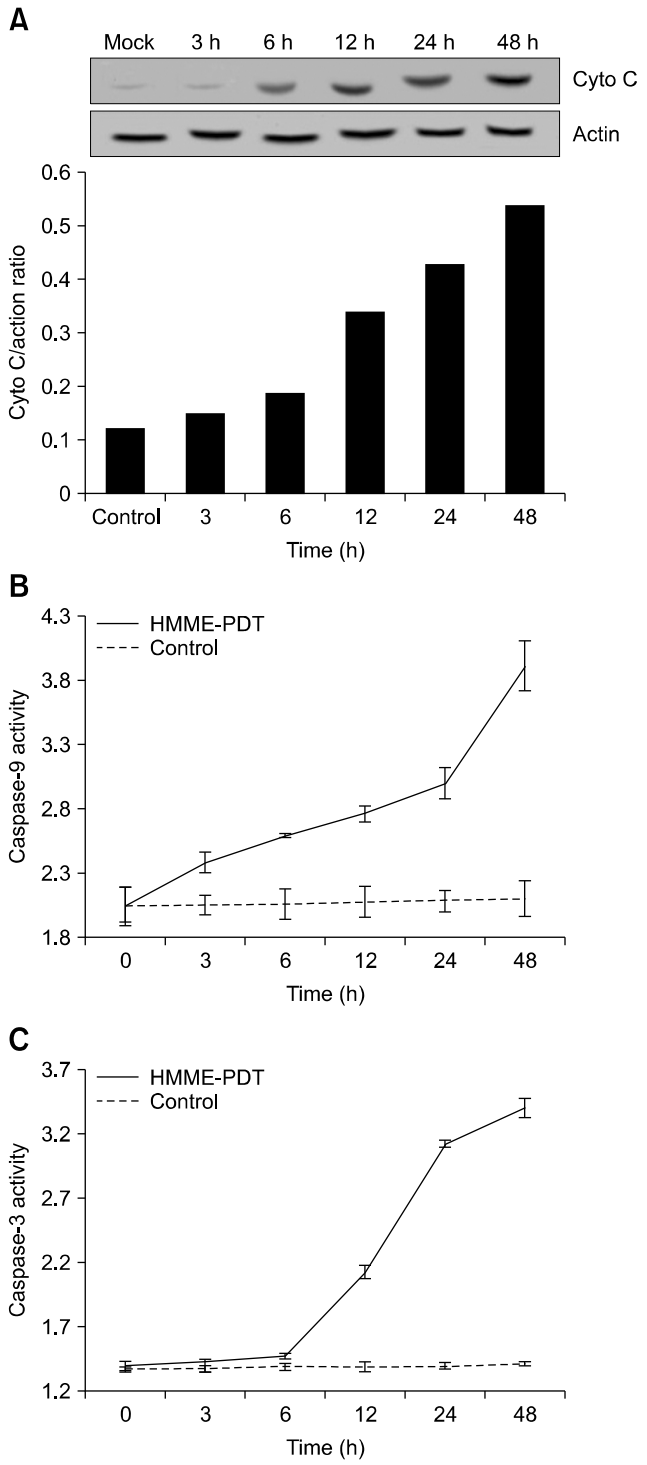


**Fig. 4.** HMME-PDT induced changes in caspase 3, 9 and Cyto C in canine breast cancer cells. (A) HMME-PDT induced the release of Cyto C at 6, 12, 24, and 48 h after PDT. (B and C) The activities of caspase-9 and caspase-3 were remarkably stimulated from 6 h and 12 h, respectively, when compared with the mock treated cells (n = 3, mean ± SD).

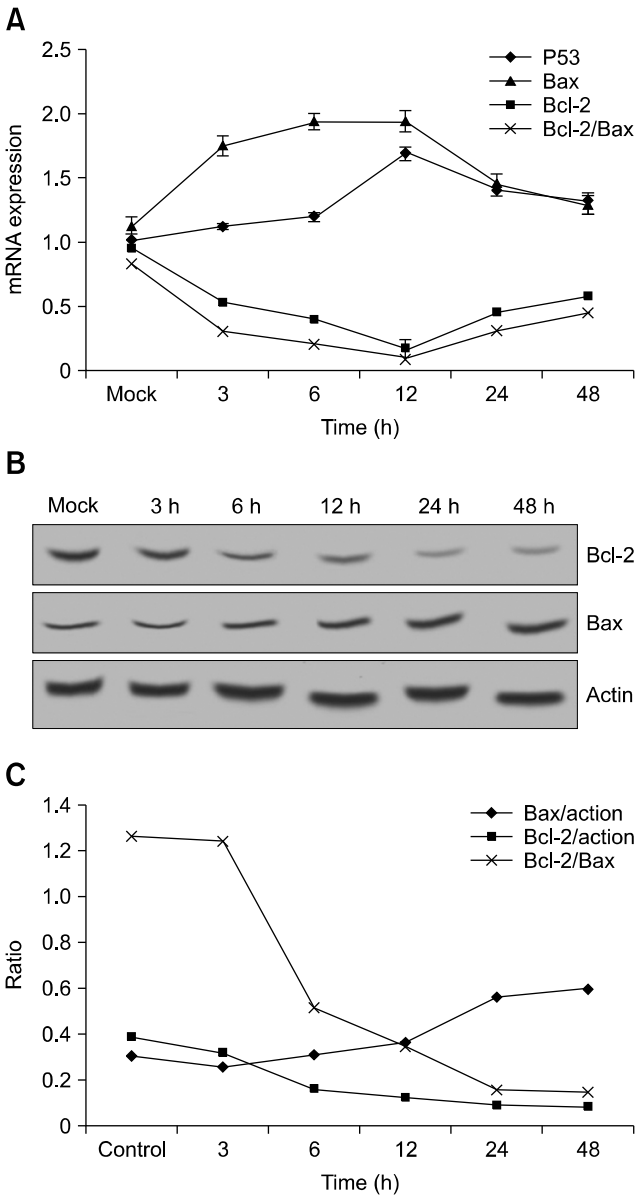


**Fig. 5.** Relative gene and protein expression in the mitochondrial apoptotic pathway. (A) The treatment up-regulated the mRNA of P53 and Bax and down-regulated Bcl-2. (B and C) Bcl-2 expression was down-regulated and Bax expression was up-regulated, further decreasing the ratio of Bcl-2 to Bax.

light irradiation using an appropriate wavelength matched to the absorption spectrum of the photosensitizer generates ROS, including singlet oxygen, superoxide anions, or hydroxyl radicals, which induce cytotoxicity [6,32,38]. HMME is mainly distributed in the cytoplasm, including mitochondria, lysosomes, endoplasmic reticulum and the Golgi apparatus [4,37]. It is the basic way that the photosensitizer localized in the mitochondria causes mitochondrial damage by PDT to induce apoptosis [16]. Mitochondria play a central role in the intrinsic pathway of

apoptosis [3]. HMME-PDT caused death of canine breast cancer cells through induced damage to the mitochondrial structure and mitochondrial dysfunction [18]. Our study demonstrated that HMME-PDT caused alterations including cytoplasmic vacuoles, cell shrinkage, and membrane blebbing, as well as cleavage of chromosomal DNA into internucleosomal fragments and cell death in canine breast cancer cells. Additionally, cell death induced in our PDT-HMME procedure was specific. These conclusions are based on the observation that massive cell death occurred in a time-dependent manner following treatment with HMME-PDT. Mitochondrial transmembrane potential was changed by HMME-PDT in canine breast cancer cells [18], inducing the permeabilization of mitochondrial membranes (MMP). MMP released several apoptogenic proteins from the inter-mitochondrial membrane space into the cytosol [3]. Mitochondrial Cyto C release into the cytosol triggers apoptosome assembly with persistently expressed Apaf-1 (apoptotic protease-activating factor) and procaspase-9. Procaspase-9 was further auto-cleaved to active Caspase-9, which in turn triggered Caspase-3 via activation of procaspase-3 [9,26]. Caspases activation also modulated the cascade of signaling transduction inside cells and controlled demolition of cellular components. Consistent with this knowledge, the results of the present study revealed that PDT-HMME treatment significantly released the mitochondrial Cyto C in the cytoplasm of the CHMm cells. The activation of caspase-9 by HMME-PDT treatment can successively stimulate procaspase-3, which in turn can activate procaspase-9 and form a positive feedback activation pathway [8]. However, as cytosolic apoptotic signals can also engage the death receptor apoptotic pathway and because the mitochondrial apoptotic pathway cross-talks with that of the death receptor [22], the death receptor pathway may also contribute to HMME-PDT-induced apoptosis in CHMm cells. Accordingly, further research is required to elucidate the detailed mechanisms of CHMm cells apoptosis induced by HMME-PDT *in vitro*.

We further evaluated the cellular apoptosis mechanism by expression of p53, Bcl-2 and Bax, which are widely accepted apoptosis indicators. As an important transcription factor, p53 is involved in apoptosis by regulating the transcription of target genes. Additionally, it is worth mentioning that the expression of p53 was found to be significantly up-regulated in CHMm cells treated with HMME-PDT in our study. These findings indicate that p53 may play a major role in the apoptosis response to HMME-PDT. The target genes of p53 encode many pro-apoptotic proteins, including PIGs, PERP, p53, AIP1, PUMA, Fas, Bax, Apaf-1, and Noxa [21]. Upon activation of apoptosis, caspase-3 can cleave p53. The fragments of p53 can then translocate to the mitochondria and induce apoptosis [30]. As a sequence-specific transcription factor, p53 induces transcription of the pro-apoptotic proteins Bax [25], while it down-regulates transcription of the anti-apoptotic proteins Bcl-2 and Bcl-x L [11]. Furthermore, p53 can directly interact with anti-apoptotic Bcl-2 and Bcl-x L proteins and suppress its function. These transcription-dependent pro-apoptotic effects of p53 may exert synergistic effects on apoptosis, rapidly amplifying the apoptotic effect and inducing the death of CHMm cells. The Bcl-2 family is pivotal in the regulation of mitochondria-initiated apoptosis [39]. Previous research has suggested that overexpression of Bcl-2 will inhibit apoptosis via the formation of Bcl-2/Bax heterodimers, and the ratio of Bcl-2 to Bax appears to play a key role in a cell's threshold for undergoing apoptosis [7]. Here, we demonstrated that HMME-PDT down-regulated Bcl-2 and up-regulated Bax expression, further decreasing the ratio of Bcl-2 to Bax. These findings indicated that HMME-PDT induces apoptosis of CHMm cells and that pro-apoptosis effects were positively correlated with Bax and Bcl-2 in the HMME-PDT-treated group. Bcl-2 is a highly sensitive target of PDT, and damage to Bcl-2 can bring about efficient induction of apoptosis [12,13]. Since the Bcl-2 family proteins play a key role in mitochondrial-dependent caspase activation [1], downregulation of Bcl-2 may cause initiation of mitochondrial apoptosis. Taken together, it is plausible that downregulation of Bcl-2 and upregulation of Bax played a major role in the HMME-PDT induced mitochondrial apoptosis pathway in CHMm cells, and that the mitochondrial apoptotic pathway plays an important role in the mechanism of HMME-PDT induced apoptosis in CHMm cells.

In summary, the present study demonstrated an anti-canine breast cancer effect of HMME-PDT *in vitro*. HMME-PDT can release Cyto C, downregulate Bcl-2, upregulate Bax and P53 and activate caspase-9, 3, thereby inducing CHMm cell apoptosis via the mitochondrial apoptosis pathway. These combined observations showed great potential for HMME-PDT in the treatment of canine breast cancer; however, the clinical relevance of these findings needs further study.

## Acknowledgments

This project was supported by the National Science Foundation of China (grant No. 31372492), the Doctoral Tutor Fund of the Ministry of Education of China (grant No. 20122325110012), and the Project of Shandong Province Higher Educational Science and Technology Program (J15LF03).

## Conflict of Interest

There is no conflict of interest.

## References

1. **Borner C.** The Bcl-2 protein family: sensors and checkpoints

for life-or-death decisions. Mol Immunol 2003, **39**, 615-647.
2. **Breen M, Modiano JF.** Evolutionarily conserved cytogenetic changes in hematological malignancies of dogs and humans − man and his best friend share more than companionship. Chromosome Res 2008, **16**, 145-154.
3. **Buytaert E, Dewaele M, Agostinis P.** Molecular effectors of multiple cell death pathways initiated by photodynamic therapy. Biochim Biophys Acta 2007, **1776**, 86-107.
4. **Dai W, Li X, Zeng J, Liu F, Gu Y.** Influence of combination form of hematoporphyrin monomethyl ether with different kinds of serum protein on its intracellular distribution. Zhongguo ji guang yi xue za zhi 2006, **3**, 137-140.
5. **Ding X, Xu Q, Liu F, Zhou P, Gu Y, Zeng J, An J, Dai W, Li X.** Hematoporphyrin monomethyl ether photodynamic damage on HeLa cells by means of reactive oxygen species production and cytosolic free calcium concentration elevation. Cancer Lett 2004, **216**, 43-54.
6. **Dougherty TJ, Gomer CJ, Henderson BW, Jori G, Kessel D, Korbelik M, Moan J, Peng Q.** Photodynamic therapy. J Natl Cancer Inst 1998, **90**, 889-905.
7. **Elmore S.** Apoptosis: a review of programmed cell death. Toxicol Pathol 2007, **35**, 495-516.
8. **Fan TJ, Han LH, Cong RS, Liang J.** Caspase family proteases and apoptosis. Acta Biochim Biophys Sin (Shanghai) 2005, **37**, 719-727.
9. **Green DR, Reed JC.** Mitochondria and apoptosis. Science 1998, **281**, 1309-1312.
10. **Haga S, Nakayama M, Tatsumi K, Maeda M, Imai S, Umesako S, Yamamoto H, Hilgers J, Sarkar NH.** Overexpression of the p53 gene product in canine mammary tumors. Oncol Rep 2001, **8**, 1215-1219.
11. **Hemann MT, Lowe SW.** The p53-Bcl-2 connection. Cell Death Differ 2006, **13**, 1256-1259.
12. **Kessel D, Castelli M.** Evidence that bcl-2 is the target of three photosensitizers that induce a rapid apoptotic response. Photochem Photobiol 2001, **74**, 318-322.
13. **Kessel D, Reiners JJ Jr.** Apoptotic response to photodynamic therapy *versus* the Bcl-2 antagonist HA14-1. Photochem Photobiol 2002, **76**, 314-319.
14. **Klopfleisch R, Lenze D, Hummel M, Gruber AD.** The metastatic cascade is reflected in the transcriptome of metastatic canine mammary carcinomas. Vet J 2011, **190**, 236-243.
15. **Kumaraguruparan R, Prathiba D, Nagini S.** Of humans and canines: immunohistochemical analysis of PCNA, Bcl-2, p53, cytokeratin and ER in mammary tumours. Res Vet Sci 2006, **81**, 218-224.
16. **Lam M, Oleinick NL, Nieminen AL.** Photodynamic therapy-induced apoptosis in epidermoid carcinoma cells. Reactive oxygen species and mitochondrial inner membrane permeabilization. J Biol Chem 2001, **276**, 47379-47386.
17. **Lee SJ, Kim MS, Park JY, Woo JS, Kim YK.** 15-Deoxy-$\Delta^{12,14}$-prostaglandin $J_2$ induces apoptosis via JNK-mediated mitochondrial pathway in osteoblastic cells. Toxicology 2008, **248**, 121-129.
18. **Li HT, Song XY, Yang C, Li Q, Tang D, Tian WR, Liu Y.** Effect of hematoporphyrin monomethyl ether-mediated PDT on the mitochondria of canine breast cancer cells. Photodiagnosis Photodyn Ther 2013, **10**, 414-421.
19. **Liu Y, Ma XQ, Jin P, Li HT, Zhang RR, Ren XL, Wang HB, Tang D, Tian WR.** Apoptosis induced by hematoporphyrin monomethyl ether combined with He-Ne laser irradiation in vitro on canine breast cancer cells. Vet J 2011, **188**, 325-330.
20. **Ma X, Jing P, Ren X, Zhang R, Liu Y.** The research of PDT to exosomatic lethal effect of canine breast tumor cells lines CHMm. Laser J 2009, **2**, 81-82.
21. **Meek DW.** The p53 response to DNA damage. DNA Repair (Amst) 2004, **3**, 1049-1056.
22. **Mignotte B, Vayssiere JL.** Mitochondria and apoptosis. Eur J Biochem 1998, **252**, 1-15.
23. **Moore KJ, Matlashewski G.** Intracellular infection by *Leishmania donovani* inhibits macrophage apoptosis. J Immunol 1994, **152**, 2930-2937.
24. **Nakagawa T, Watanabe M, Ohashi E, Uyama R, Takauji S, Mochizuki M, Nishimura R, Ogawa H, Sugano S, Sasaki N.** Cyclopedic protein expression analysis of cultured canine mammary gland adenocarcinoma cells from six tumours. Res Vet Sci 2006, **80**, 317-323.
25. **Nakamura Y.** Isolation of p53-target genes and their functional analysis. Cancer Sci 2004, **95**, 7-11.
26. **Newmeyer DD, Ferguson-Miller S.** Mitochondria: releasing power for life and unleashing the machineries of death. Cell 2003, **112**, 481-490.
27. **Pfaffl MW.** A new mathematical model for relative quantification in real-time RT-PCR. Nucleic Acids Res 2001, **29**, e45.
28. **Pinho SS, Carvalho S, Cabral J, Reis CA, Gärtner F.** Canine tumors: a spontaneous animal model of human carcinogenesis. Transl Res 2012, **159**, 165-172.
29. **Pinthus JH, Bogaards A, Weersink R, Wilson BC, Trachtenberg J.** Photodynamic therapy for urological malignancies: past to current approaches. J Urol 2006, **175**, 1201-1207.
30. **Sayan BS, Sayan AE, Knight RA, Melino G, Cohen GM.** p53 is cleaved by caspases generating fragments localizing to mitochondria. J Biol Chem 2006, **281**, 13566-13573.
31. **Setoguchi A, Sakai T, Okuda M, Minehata K, Yazawa M, Ishizaka T, Watari T, Nishimura R, Sasaki N, Hasegawa A, Tsujimoto H.** Aberrations of the p53 tumor suppressor gene in various tumors in dogs. Am J Vet Res 2001, **62**, 433-439.
32. **Sharman WM, Allen CM, van Lier JE.** Photodynamic therapeutics: basic principles and clinical applications. Drug Discov Today 1999, **4**, 507-517.
33. **Song K, Kong B, Li L, Yang Q, Wei Y, Qu X.** Intraperitoneal photodynamic therapy for an ovarian cancer ascite model in Fischer 344 rat using hematoporphyrin monomethyl ether. Cancer Sci 2007, **98**, 1959-1964.
34. **Thomas R, Smith KC, Ostrander EA, Galibert F, Breen M.** Chromosome aberrations in canine multicentric lymphomas detected with comparative genomic hybridisation and a panel of single locus probes. Br J Cancer 2003, **89**, 1530-1537.
35. **Uva P, Aurisicchio L, Watters J, Loboda A, Kulkarni A, Castle J, Palombo F, Viti V, Mesiti G, Zappulli V, Marconato L, Abramo F, Ciliberto G, Lahm A, La Monica N, de Rinaldis E.** Comparative expression pathway analysis of human and canine mammary tumors. BMC Genomics 2009, **10**, 135.

36. **Walker JM.** The bicinchoninic acid (BCA) assay for protein quantitation. Methods Mol Biol 1994, **32**, 5-8.
37. **Wang L, Dai W, Li J, Liu F, Gu Y, Li X, Zheng J.** Quantitative study of HMME subcellular localization via confocal fluorescence microscopy. Laser J 2004, **2**, 77-79.
38. **Wilson BC.** Photodynamic therapy for cancer: principles. Can J Gastroenterol 2002, **16**, 393-396.
39. **Yang WY, Liu CH, Chang CJ, Lee CC, Chang KJ, Lin CT.** Proliferative activity, apoptosis and expression of oestrogen receptor and Bcl-2 oncoprotein in canine mammary gland tumours. J Comp Pathol 2006, **134**, 70-79.